# Substitution of a Single Residue in *Stichodactyla helianthus* Peptide, ShK-Dap$^{22}$, Reveals a Novel Pharmacological Profile

Richard E. Middleton,[‡,§] Manuel Sanchez,[‡,§] Ana-Rosa Linde,[‡,§,||] Randal M. Bugianesi,[‡] Ge Dai,[‡] John P. Felix,[‡] Sam L. Koprak,[⊥] Mary Jo Staruch,[⊥] Marc Bruguera,[‡] Rachael Cox,[‡] Amrita Ghosh,[‡] Jeremy Hwang,[‡] Simmonette Jones,[‡] Martin Kohler,[‡] Robert S. Slaughter,[‡] Owen B. McManus,[‡] Gregory J. Kaczorowski,[‡] and Maria L. Garcia*[,‡]

*Departments of Ion Channels and Immunology Research, Merck Research Laboratories, P.O. Box 2000, Rahway, New Jersey 07065*

*Received July 9, 2003; Revised Manuscript Received September 15, 2003*

ABSTRACT: ShK, a peptide isolated from *Stichodactyla helianthus* venom, blocks the voltage-gated potassium channels, $K_v1.1$ and $K_v1.3$, with similar high affinity. ShK-Dap$^{22}$, a synthetic derivative in which a diaminopropionic acid residue has been substituted at position Lys$^{22}$, has been reported to be a selective $K_v1.3$ inhibitor and to block this channel with equivalent potency as ShK [Kalman et al. (1998) *J. Biol. Chem. 273*, 32697−32707]. In this study, a large body of evidence is presented which indicates that the potencies of wild-type ShK peptide for both $K_v1.3$ and $K_v1.1$ channels have been previously underestimated. Therefore, the affinity of ShK-Dap$^{22}$ for both channels appears to be ca. $10^2-10^4$-fold weaker than ShK. ShK-Dap$^{22}$ does display ca. 20-fold selectivity for human $K_v1.3$ vs $K_v1.1$ when measured by the whole-cell voltage clamp method but not in equilibrium binding assays. ShK-Dap$^{22}$ has low affinity for $K_v1.2$ channels, but heteromultimeric $K_v1.1$-$K_v1.2$ channels form a receptor with ca. 200-fold higher affinity for ShK-Dap$^{22}$ than $K_v1.1$ homomultimers. In fact, $K_v1.1$-$K_v1.2$ channels bind ShK-Dap$^{22}$ with only ca. 10-fold less potency than ShK and reveal a novel pharmacology not predicted from the homomultimers of $K_v1.1$ or $K_v1.2$. The concentrations of ShK-Dap$^{22}$ needed to inhibit human T cell activation were ca. $10^3$-fold higher than those of ShK, in good correlation with the relative affinities of these peptides for inhibiting $K_v1.3$ channels. All of these data, taken together, suggest that ShK-Dap$^{22}$ will not have the same in vivo immunosuppressant efficacy of other $K_v1.3$ blockers, such as margatoxin or ShK. Moreover, ShK-Dap$^{22}$ may have undesired side effects due to its interaction with heteromultimeric $K_v1.1$-$K_v1.2$ channels, such as those present in brain and/or peripheral tissues.

Peptides isolated from scorpion, snake, and sea anemone venoms have become invaluable tools for studying the outer pore structure of potassium channels (*1*). From the sea anemone venoms *Stichodactyla helianthus* and *Bunodosoma granulifera*, two peptides, ShK[1] and BgK, have been purified and characterized (*2*, *3*). ShK and BgK contain 35 and 37 amino acid residues, respectively, and block with different potencies and selectivities a subset of voltage-gated potassium channels of the $K_v1.x$ family. ShK is a high-affinity blocker of $K_v1.1$ and $K_v1.3$ channels, whereas BgK blocks with similar potency $K_v1.1$, $K_v1.2$, and $K_v1.3$ channels. The three-dimensional structure of these peptides, containing a central helix−kink−helix fold, is quite different from that of the $K_v1$ scorpion channel blocking peptides (*4*). Despite this fact, all of these pore-blocking peptides appear to use a common functional diad for blocking the channel, consisting of a lysine and a hydrophobic residue, separated by about 7 Å (*5*). Substitution of the critical lysine$^{22}$ residue of ShK with the unnatural amino acid, diaminopropionic acid (ShK-Dap$^{22}$), has been reported to weaken the resulting peptide's affinity for $K_v1.1$ ca. 100-fold but to have no significant effect on $K_v1.3$ channel blocking potency (*6*). Thus, ShK-Dap$^{22}$ has been proposed to be a selective $K_v1.3$ inhibitor. A similar substitution in BgK led to >100-fold decrease in the potency of the resulting peptide for all three BgK-sensitive channels, $K_v1.1$, $K_v1.2$, and $K_v1.3$ (*7*).

The discovery of selective $K_v1.3$ inhibitors is of interest, given the critical role that $K_v1.3$ plays in human T lymphocyte activation. In human T lymphocytes, $K_v1.3$ sets the resting potential, and its inhibition causes cell depolarization, leading to attenuation in the rise of intracellular calcium levels that occurs upon T cell receptor stimulation, which is necessary for T cell proliferation (*8*, *9*). In addition, $K_v1.3$ channels appear to be specifically upregulated in activated human effector memory cells, suggesting a role for this channel in autoimmune diseases (*10*). Peptides and small

* To whom correspondence should be addressed at P.O. Box 2000, RY80N-C31, Rahway, NJ 07065. Tel: 732-594-7564. Fax: 732-594-3925. E-mail: maria_garcia@merck.com.

‡ Department of Ion Channels, Merck Research Laboratories.

§ Contributed equally to this work.

|| Present address: National School of Public Health, Oswaldo Cruz Foundation, Brazil.

⊥ Immunology Research, Merck Research Laboratories.

[1] Abbreviations: $K_v$, voltage-gated potassium channel; $^{125}$I-HgTX$_1$-A19Y/Y37F, monoiodotyrosine-hongotoxin$_1$-A19Y/Y37F; $K_d$, equilibrium dissociation constant; $K_i$, equilibrium inhibition constant; MgTX, margatoxin; ShK, *Stichodactyla helianthus* peptide; ShK-Dap$^{22}$, *Stichodactyla helianthus* lysine$^{22}$-diaminopropionic acid; VIPR, voltage/ion probe reader; PBMC, peripheral blood mononuclear cells.

10.1021/bi035209e CCC: $25.00 
Published on Web 11/01/2003

molecule $K_v1.3$ blockers have been shown to have immunosuppressant activity in in vivo animal models (*11*−*14*).

In this study, evidence is presented which indicates that the potency of ShK-Dap$^{22}$ for human $K_v1.3$ is >100-fold weaker than ShK. This was observed in five different cell-based assays. ShK-Dap$^{22}$ does block current through $K_v1.3$ about 20-fold more potently than human $K_v1.1$ channels, but in equilibrium binding studies, it binds to both channels with similar affinity. Although ShK-Dap$^{22}$ displays low potency for $K_v1.2$ channels, it binds with relatively high affinity to $K_v1.1$-$K_v1.2$ heteromultimers compared to homomultimeric $K_v1.1$ channels. Given the unexpected pharmacological profile of ShK-Dap$^{22}$ for heteromultimeric $K_v1.1$-$K_v1.2$ channels and greatly reduced potency on $K_v1.3$, ShK-Dap$^{22}$ is not predicted to have the efficacy or specificity that is needed for its development as an immunosuppressant. A preliminary report of these findings has been presented in abstract form (*15*).

## EXPERIMENTAL PROCEDURES

*Materials*. Restriction enzymes and the pCI-neo vector were bought from Promega. The pEGFP-N1 vector was from Clontech, and *Pfu* DNA polymerase was from Stratagene. The TsA-201 cell line, a subclone of the human embryonic kidney cell line HEK293 that expresses the SV40 T antigen, was a gift of Dr. Robert DuBridge. All tissue culture media were from Gibco, serum was from Hyclone, and the FuGENE6 transfection reagent was from Boehringer Mannheim. $^{86}$RbCl and [$^3$H]thymidine (6.7 Ci/mmol) were purchased from NEN Life Science Products. CHO cells stably transfected with the human $K_v1.3$ channel were prepared as previously described (*16*). HEK293 cells stably transfected with homotetrameric human $K_v1.1$ and $K_v1.3$ channels were obtained from Professor Olaf Pongs (Zentrum für Molekulare Neurobiologie, Hamburg, Germany), whereas those transfected with homotetrameric human $K_v1.2$ channels were obtained as previously described (*17*). Human brain tissue was provided by Drs. H.-G. Knaus and H. Glossmann, University of Innsbruck, Innsbruck, Austria. ShK was purchased from Peptides International. Hongotoxin$_1$-A19Y/Y37F (HgTX$_1$A19Y/Y37F) was prepared and radioiodinated as described (*18*). CC2-DMPE and DiSBAC$_2$(3) were bought from Panvera (Madison, WI), and pluronic acid was from Molecular Probes (Eugene, OR). Human T cell conditioned medium was from Collaborative Research (Cambridge, MA). OKT3 (anti-CD3) mAb was obtained from Ortho Diagnostic Systems (Raritan, NJ). GF/C glass fiber filters were obtained from Whatman, and poly(ethylenimine) was from Sigma. All other reagents were obtained from commercial sources and were of the highest purity available.

*$K_v1.1$-$K_v1.2$ Dimer and Tetramer Constructs*. cDNA coding for a $K_v1.1$-$K_v1.2$ dimer was prepared as previously described (*3*). To obtain a $K_v1.1$-1.2-1.1-1.2 construct, the $K_v1.1$-1.2 dimer in pCI-neo served as starting material. The insert of the dimer plasmid was amplified by PCR (Pfu Turbo, Stratagene) with the following primer pair: $K_v1.1$Nhe-s, GCATGCTAGCACGCCACCATGACGGTGATGTCTGGGGAG, and $K_v1.2$BspE-as, CGTATCCGGAGACATCAGTTAACATTTTGG. The resulting fragment was subcloned into pCI-neo and sequenced to ensure the correctness of the amplified dimer. The dimer was amplified with a second primer pair: h$K_v1.1$Q10BspE, GCTATCCGGACAACAGCAGCAACAACAGCAGCAACAACAGATGACGGTGATGTCTGGGGAG, and h$K_v1.2$op-Mlu-as, GCTAACGCGTTCAGACATCAGTTAACATTTTGG. The product of this PCR reaction was also subcloned in pCI-neo and sequenced.

The $K_v1.1$-1.2-1.1-1.2 tetramer was constructed by joining a dimer fragment with *Nhe*I and *Bsp*EI restriction sites at its 5′ and 3′ ends, respectively, from the first PCR reaction, with a dimer fragment from the second PCR reaction with *Bsp*EI and *Mlu*I sites at the 5′ and 3′ ends. The pCI expression vector (Promega) was prepared with the restriction enzymes *Nhe*I and *Mlu*I. The product of this ligation reaction was introduced into STBL2-competent cells (Invitrogen). A plasmid with the desired tetramer was chosen on the basis of the expected restriction pattern.

*Synthesis of ShK-Dap$^{22}$*. ShK-Dap$^{22}$ was prepared by solid-phase synthesis by Peptides International. The folded peptide was characterized by amino acid hydrolysis (Peptides International), HPLC, amino acid sequencing (Porton Instruments PI2090E), and mass spectroscopy. The mass contents of ShK and ShK-Dap$^{22}$ solutions were determined by amino acid hydrolysis. Solutions of the peptides were made in 100 mM NaCl, 20 mM Tris-HCl, pH 7.4, and 0.1% bovine serum albumin. Aliquots were frozen in liquid $N_2$ and stored at −70 °C. Once thawed, the solutions were kept at 4 °C.

*Human T Cell Preparation*. Human peripheral blood mononuclear cells (PBMC) were isolated as previously indicated (*13*). Purified T cells were prepared by rosetting as described (*13*). Purity of human T cells was 95−97%, as determined by anti-CD3 staining in FACS analyses.

*Electrophysiological Recordings from Human T Lymphocytes*. Whole-cell recordings were made from purified human T lymphocytes as previously described using standard methods (*19*). Electrodes were pulled from Garner 7052 glass; their resistances were 1−3 mΩ when filled with standard pipet solution and immersed in bath solution. The pipet contained 120 mM KCl, 20 mM KF, 10 mM Hepes, and 10 mM $K_2$EGTA, pH 7.2, with KOH, and the bath solution contained 160 mM NaCl, 10 mM Hepes, 4.5 mM KCl, 2 mM $CaCl_2$, and 1 mM $MgCl_2$, pH 7.2, with NaOH. The amplifier inputs were connected to the experimental solutions via Ag/AgCl electrodes, and the bath electrode contacted the bath solution through an agar bridge containing 200 mM KCl. No corrections for junction potentials or series resistance were applied. Experiments were done under constant flow (1−2 mL/min) with a chamber volume of 0.2−0.4 mL at room temperature (22−24 °C).

Membrane currents were measured with Axopatch 1D (Axon Instruments) or EPC9 (HEKA Electronik) amplifiers. Voltage control and data acquisition were done using ITC-16 interfaces (Instrutech Corp.) connected to Macintosh computers (Apple Computer) running Pulse software (HEKA Electronik). Data analysis was done using PulseFit (HEKA Electronik) and Igor Pro (Wavemetrics Inc.) software. Currents were filtered at 2−5 kHz and digitized at 5−10 kHz. Analogue capacity compensation was applied, and digital compensation of the leak and residual capacity currents was done using a P/-4 protocol from the standard holding potential (−80 mV), with subtraction pulses applied 4−10 s after the test pulses. If peak current amplitudes were stable in the control for 10 min or more, peptides were applied until a steady-state level of block was reached. Mean

inhibition values (±SEM) at each peptide concentration were fit with Hill equations with the slope fixed to 1.

*Electrophysiological Recordings from Xenopus Oocytes*. *Xenopus* oocytes were injected with 50 nL of water containing 0.5−5 ng of RNA encoding human $K_v1.1$ or $K_v1.3$ channel proteins and stored at 18 °C. Membrane currents were recorded 1−5 days after injection using standard two-electrode voltage clamp methods. Currents were recorded with a Dagan CA-1 (Dagan Corp.) oocyte clamp. Data acquisition and analysis were done as described above for the experiments using T lymphocytes. Electrodes were filled with 2 M KCl, and current injection electrodes had resistances of 0.3−0.8 MΩ. Oocytes with peak current amplitudes in the range of 1−5 μA were typically used. Recordings were made at room temperature (22−24 °C) in a 0.5 mL chamber with constant superfusion at 1−1.5 mL/min. Steady-state levels of channel block were calculated for each oocyte, and mean values (±SEM) at each peptide concentration were fit with Hill equations as described above.

*$^{86}Rb^+$ Efflux Assay*. The $^{86}Rb^+$ efflux assay is a modified form of a previously described technique (*16*, *19*). CHO cells stably expressing human $K_v1.3$ are preincubated in 12-well plates overnight in the presence of trace amounts of $^{86}Rb^+$ in 1.5 mL of growth media. Triplicate samples of 2.5 mL peptide solutions in low K buffer (in mM: 135 NaCl, 4.6 KCl, 1 $CaCl_2$, 20 Hepes, pH 7.4, with NaOH) with 2 mM glucose and 1% bovine serum albumin were added to each well. After at least 1 h incubation at 37 °C, each well was washed three times with 3.33 mL of low K buffer, and then 2 mL of high K buffer (in mM: 140 KCl, 1 $CaCl_2$, 2 $MgCl_2$, 10 Hepes-K, pH 7.4) was added. After 12 min, the high K buffer was removed and placed in a 20 mL vial containing 10 mL of scintillation fluid. Two milliliters of 1% sodium dodecyl sulfate was added to each well to rupture the cell membrane prior to counting the remaining intracellular $^{86}Rb^+$. After approximately 1 h, the 2 mL sodium dodecyl sulfate solution was removed, placed in a vial with 10 mL of scintillation fluid, and analyzed by liquid scintillation techniques. Efflux was defined as the percent of $^{86}Rb^+$ in each well that was present in the 2 mL high K buffer.

*Transfection of TsA-201 Cells and Membrane Preparation*. The procedures for handling TsA-201 cells, their transfection with FuGENE6 transfection reagent, and preparation of membrane vesicles have been previously described (*17*). The final membrane pellet was resuspended in 100 mM NaCl and 20 mM Hepes−NaOH, pH 7.4. Aliquots were frozen in liquid $N_2$ and stored at −70 °C.

*$^{125}I$-HgTX$_1$A19Y/Y37F Binding*. The interaction of $^{125}I$-$HgTX_1$A19Y/Y37F with human $K_v1.x$ channels was determined in a medium consisting of 100 mM NaCl, 5 mM KCl, 20 mM Tris-HCl, pH 7.4, and 0.1% bovine serum albumin. A total volume of 12 mL was used in order to maintain the receptor concentration below the determined $IC_{50}$ values of inhibition. Incubations were carried out for 20 h at room temperature. Separation of bound from free $^{125}I$-$HgTX_1$-A19Y/Y37F was achieved using filtration protocols as described (*18*). Nonspecific binding was determined in the presence of 1 nM margatoxin (MgTX).

*Membrane Potential Assay*. CHO cells stably expressing $K_v1.3$ were plated in black-wall, clear-bottom 96-well plates and grown overnight in growth media to reach confluency prior to assay on VIPR (ca. $1 \times 10^5$ cells/well). Cells were washed with 200 μL of Dulbecco's phosphate-buffered saline supplemented to 10 mM glucose and 10 mM Hepes-Na, pH 7.2 (DPBS), and then incubated in 100 μL of 5 μM CC2-DMPE and 0.02% pluronic acid in DPBS for 30−60 min at room temperature. Wells were rinsed twice with 100 μL of sodium gluconate (in mM: 150 sodium gluconate, 4 KCl, 1 $CaCl_2$, 0.5 $MgCl_2$, 11 glucose, 20 sodium phosphate, pH 7.2) and then incubated in 100 μL of sodium gluconate supplemented with 10 μM $DiSBAC_2(3)$ and test sample at the indicated concentration for 30−60 min at room temperature. At the end of this incubation, the plate was placed in the VIPR reader, illuminated at 400 nm, and fluorescence emissions at 460 and 580 nm were recorded. After a 7 s baseline reading, 100 μL of potassium gluconate solution was added (in mM: 150 potassium gluconate, 4 KCl, 1 $CaCl_2$, 0.5 $MgCl_2$, 11 glucose, 20 sodium phosphate, pH 7.2). The change in membrane potential was detected as the change in fluorescence resonance energy transfer, determined as the ratio, $F/F_0$, or more explicitly as

$$F/F_0 = (M_{480}/M_{560})/(I_{480}/I_{560})$$

where $M$ and $I$ are maximal and initial fluorescence emission measurements at the indicated wavelengths.

*Data Analysis*. Data from saturation experiments were analyzed according to the equation $B_{eq} = (B_{max}L^*)/(K_d + L^*)$, where $B_{eq}$ is the amount of ligand bound at equilibrium, $B_{max}$ the maximum receptor concentration, $K_d$ the ligand dissociation constant, and $L^*$ the free ligand concentration. $IC_{50}$ values for inhibition of $^{125}I$-$HgTX_1$A19Y/Y37F binding were determined using the equation $B_{eq} = (B_{max} - B_{min})/[1 + (I/IC_{50})^{nH}] + B_{min}$, where $B_{max}$ is the binding with no inhibitors present, $B_{min}$ is the minimum amount of ligand bound at the maximal inhibitor concentration, $I$ is the inhibitor concentration, $nH$ is the Hill coefficient, and $IC_{50}$ is the inhibition constant. For the data, $B_{max}$ was usually around 100% and $B_{min}$ was 0%. Inhibition of $^{125}I$-$HgTX_1$-A19Y/Y37F binding to $K_v1.1$-1.2 dimer and $K_v1.1$-1.2-1.1-1.2 membranes by ShK-Dap$^{22}$ was analyzed according to the equation $B_{eq} = (B_{max} - B_{min})/[1 + (I/IC_{50(1)})^{nH1}] + B_{min}/[1 + (I/IC_{50(2)})^{nH2}]$, where the parameters corresponding to sites 1 and 2 are described above.

*Proliferation Assays*. Purified human T lymphocytes were cultured in 96-well microtiter plates (Costar, Cambridge, MA) as described (*13*). Compounds were added and incubated for 15−30 min at 37 °C. The cultures were stimulated with 0.3 ng/mL OKT3. Irradiated (1500 R) autologous PBMC cells were then added, and cultures were incubated for 3 days at 37 °C as described (*13*). T cell proliferation was measured by addition of 2 μCi/well [$^3H$]thymidine about 18 h before harvesting. Cultures were harvested, and radioactivity associated with filters was determined by liquid scintillation techniques. The data shown represent the means of triplicate wells.

## RESULTS

*ShK-Dap$^{22}$ Blocks $K_v$ Channels in Human T Cells Less Potently Than ShK*. ShK has previously been characterized as a high-affinity blocker of $K_v1.1$ and $K_v1.3$ channels (*6*). $K_v1.3$ inhibitors have shown efficacy in suppressing immune responses in in vitro experiments (*6*, *13*, *14*, *19*−*23*) and in in vivo models (*11*−*14*). Consistent with this, ShK inhibits

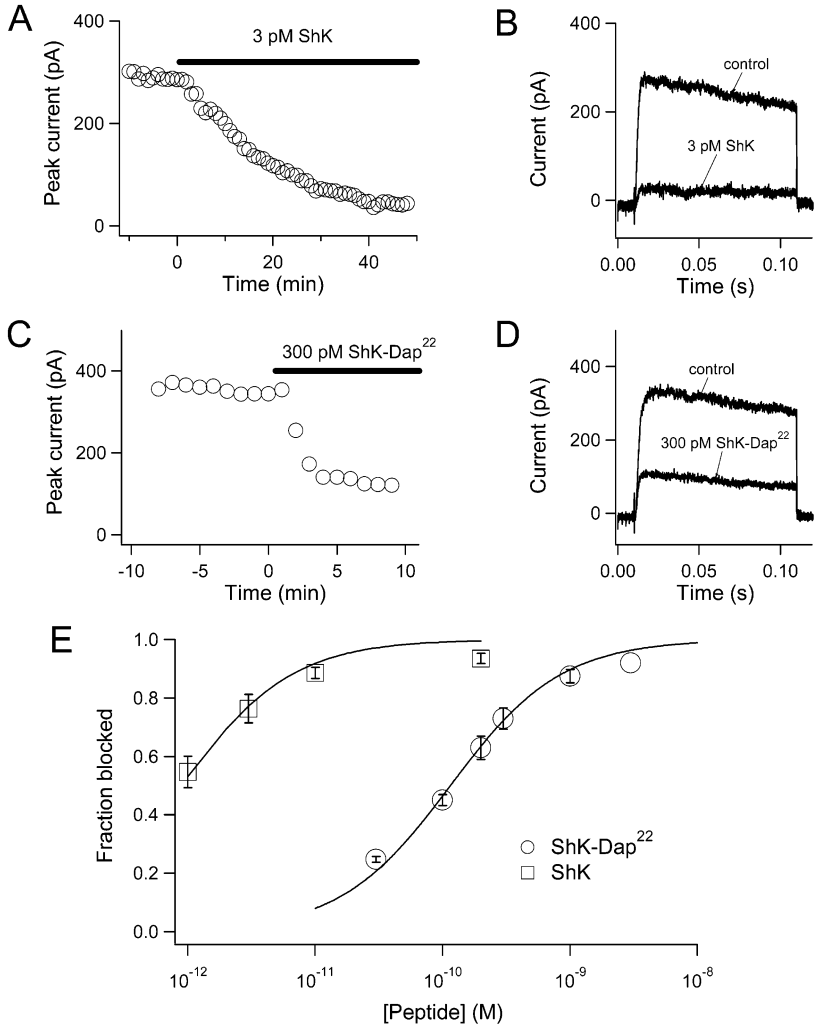


FIGURE 1: Block of $K_v1.3$ channels in human T lymphocytes by ShK and ShK-Dap$^{22}$. The time course of channel block by 3 pM ShK is shown in (A), and membrane currents recorded in control and after 45 min in ShK are shown in (B). (C) shows the time course of block after 300 pM ShK-Dap$^{22}$, and (D) shows currents recorded in control and after 9 min in 300 pM ShK-Dap$^{22}$. The steady-state fraction of channels blocked was estimated for each experiment, and mean values are plotted against peptide concentration in (E). Mean values were calculated from three to ten determinations at each peptide concentration, except one determination was made at 3000 pM ShK-Dap$^{22}$ and two determinations were made at 1 pM ShK.

human T cell proliferation (*6*, *10*) and can prevent and ameliorate experimental autoimmune encephalomyelitis (*11*, *12*). Thus, a selective $K_v1.3$ inhibitor could provide a potential immunosuppressive therapy. Toward this end, it was reported that substitution of diaminopropionic acid at the critical Lys$^{22}$ residue generates a peptide, ShK-Dap$^{22}$, that retains the same affinity for $K_v1.3$ as ShK but with 100-fold reduced potency against the $K_v1.1$ channel (*6*). To evaluate the efficacy of these peptides, ShK and ShK-Dap$^{22}$ peptides were synthesized by solid-phase synthesis and folded, and their structures were confirmed by a number of analytical techniques.

Inhibition of $K_v1.3$ channels in human T lymphocytes by ShK and ShK-Dap$^{22}$ was investigated using whole-cell, voltage clamp recording methods (Figure 1). T cells were held at a membrane potential of −80 mV, and the peak outward potassium current was measured during 100 ms voltage steps to +20 mV, delivered once per minute. Currents were blocked by both peptides. Figure 1A shows the time course of channel block by 3 pM ShK. Block equilibrated along an exponential time course with a time constant of 20 min, and a steady-state level of block (fraction blocked = 0.75) was reached after 45 min. The prolonged time course of channel block seen in Figure 1A is simply due to the low toxin concentration applied. The rate constant for channel block (ca. $7 \times 10^7$ $M^{-1}$ $s^{-1}$) was estimated from the slope of the inverse time constant for onset of block. In fact, this on-rate was somewhat higher than typical values reported for peptide−channel interactions (*24*−*30*). Due to the time required to reach steady-state block at low peptide concentration, we did not attempt to use ShK at concentrations below 1 pM (equilibration time ≥1 h). A fit of the titration of $K_v1.3$ channel block by ShK concentrations greater than 1 pM gives an estimated $IC_{50}$ value of ∼0.9 pM (Figure 1E).

In contrast to ShK, ShK-Dap$^{22}$ blocked T lymphocyte potassium currents at 100-fold higher concentrations. Application of 300 pM ShK-Dap$^{22}$ (Figure 1C,D) caused a similar level of channel block (fraction blocked = 0.65) as 3 pM ShK. The onset of channel block by 300 pM ShK-Dap$^{22}$ equilibrated in 3−4 min, as expected at a higher peptide concentration. The observed rates for channel block at 30 and 100 pM suggest that the binding rate for ShK-Dap$^{22}$ is slower (data not shown). Titration of T cell

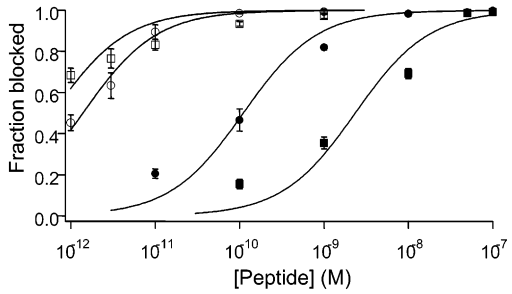


FIGURE 2: Block of $K_v1.1$ and $K_v1.3$ channels expressed in *Xenopus* oocytes by ShK and ShK-Dap$^{22}$. Block of $K_v1.1$ currents (□, ■) and $K_v1.3$ currents (○, ●) by ShK (□, ○) and ShK-Dap$^{22}$ (■, ●) is shown as a function of peptide concentration. The solid lines show fits to data with Hill equations. The $IC_{50}$'s determined for block of $K_v1.3$ by ShK and ShK-Dap$^{22}$ were 1.4 and 110 pM, respectively, and for block of $K_v1.1$ by ShK and ShK-Dap$^{22}$ 0.6 and 2300 pM, respectively. Mean values were calculated from four to eight determinations except for the value at 10 nM ShK-Dap$^{22}$ applied to $K_v1.3$ channels, which was based on two determinations.

potassium channel block by ShK-Dap$^{22}$ gave an $IC_{50}$ of 115 pM (Figure 1E), indicating that ShK-Dap$^{22}$ is at least 100-fold less potent than the parent ShK peptide. Given the technical difficulties associated with accurate measurements of steady-state block at concentrations <1 pM, the difference in potencies between both peptides could be >100-fold.

*Expression of $K_v1.1$ and $K_v1.3$ Channels in Xenopus Oocytes: Sensitivity to ShK and ShK-Dap$^{22}$.* To examine the selectivity of ShK and ShK-Dap$^{22}$ for blocking $K_v1.3$ channels compared with block of related voltage-gated potassium channels, voltage clamp recordings were made with *Xenopus* oocytes expressing human $K_v1.3$ and $K_v1.1$ channels. Figure 2 shows titrations of steady-state block of $K_v1.3$ and $K_v1.1$ channels by ShK and ShK-Dap$^{22}$. In harmony with the results obtained using human T lymphocytes (Figure 1), $K_v1.3$ channels expressed in *Xenopus* oocytes were blocked by ShK with an $IC_{50}$ of 1.4 pM and by ShK-Dap$^{22}$ at 100-fold higher concentrations ($IC_{50}$ = 110 pM). $K_v1.1$ channels were blocked by ShK ($IC_{50}$ = 0.6 pM) with similar potency, although these measurements were at the limit of determination in electrophysiological experiments. In contrast to the nearly 100-fold decrease in affinity observed for $K_v1.3$ channels, modification of ShK to ShK-Dap$^{22}$ caused a nearly 4000-fold decrease in affinity for $K_v1.1$ channels. Therefore, ShK-Dap$^{22}$ is less potent than ShK toxin on both channels but displays a 20-fold selectivity for block of human $K_v1.3$ over $K_v1.1$ channels, while native ShK peptide shows little selectivity.

*$^{86}Rb^+$ Flux through $K_v1.3$ Channels: Effect of ShK and ShK-Dap$^{22}$.* An alternative method for evaluating the activity of $K_v1.3$ channels is to measure depolarization-induced $^{86}Rb^+$ efflux from cells stably expressing the channel (*16*, *19*). For this purpose, CHO cells stably expressing the human $K_v1.3$ channel are loaded with $^{86}Rb^+$, and a high potassium solution is used to cause depolarization and open the channels. MgTX inhibits $^{86}Rb^+$ efflux through $K_v1.3$ channels with an $IC_{50}$ = 25 pM (Figure 3). ShK displays a similar high potency in this assay, $IC_{50}$ = 10 pM. In contrast, ShK-Dap$^{22}$ is a less potent inhibitor of $K_v1.3$ channels with an $IC_{50}$ = 4500 pM, which is ca. 500-fold weaker than that of ShK. Although the apparent potency of the peptides in the $^{86}Rb^+$ efflux assay is lower than in electrophysiological assays (see Discussion), a similar difference in rank order of potency between ShK and ShK-Dap$^{22}$ is present in both protocols.

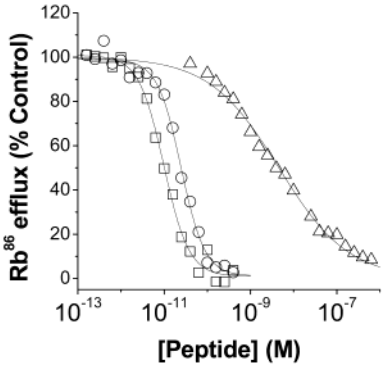


FIGURE 3: $^{86}Rb^+$ flux through $K_v1.3$: effect of ShK and ShK-Dap$^{22}$. HEK293 cells that stably express $K_v1.3$ were incubated overnight in the presence of trace amounts of $^{86}Rb^+$. The cells were then preincubated with the indicated concentration of peptide for 1 h with $^{86}Rb^+$. Depolarization-induced efflux was initiated by addition of 140 mM KCl, and incubation was carried out at room temperature. After 12 min, efflux was measured as the ratio of the $^{86}Rb^+$ in the bath divided by the total $^{86}Rb^+$. Percent inhibition was defined according to the maximal produced by 10 nM MgTX. The data were fit to $IC_{50}$ values of 24.7, 9.9, and 4530 pM for MgTX (○), ShK (□), and ShK-Dap$^{22}$ (△), respectively.

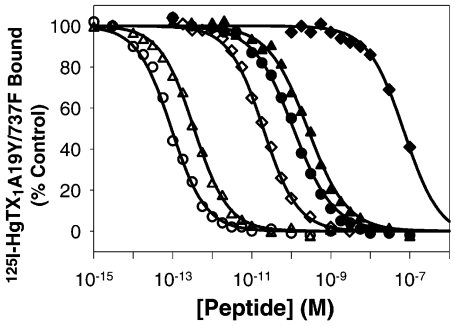


FIGURE 4: Binding of $^{125}$I-HgTX$_1$A19Y/Y37F to $K_v1.1$, $K_v1.2$ or $K_v1.3$: effect of ShK and ShK-Dap$^{22}$. Membranes prepared from HEK293 cells stably expressing human $K_v1.1$ (○, ●), $K_v1.2$ (◇, ◆), or $K_v1.3$ (△, ▲) channels were incubated with ~0.1 pM $^{125}$I-HgTX$_1$A19Y/Y37F, in the absence or presence of increasing concentrations of either ShK (open symbols) or ShK-Dap$^{22}$ (closed symbols), for 20 h at room temperature. The incubation medium consisted of 100 mM NaCl, 5 mM KCl, 20 mM Tris-HCl, pH 7.4, and 0.1% bovine serum albumin. Nonspecific binding was determined in the presence of 1 nM MgTX. Specific binding data are presented relative to an untreated control. It was critical to maintain a receptor site density below 0.1 pM to ensure accurate determinations of $K_i$ values.

*Binding of $^{125}$I-HgTX$_1$A19Y/Y37F to $K_v1.1$, $K_v1.2$, and $K_v1.3$ Channels: Effect of ShK and ShK-Dap$^{22}$.* Under equilibrium conditions, $^{125}$I-HgTX$_1$A19Y/Y37F binds with high affinity to membranes derived from HEK293 cells stably transfected with human $K_v1.1$, $K_v1.2$, or $K_v1.3$ channels. The equilibrium dissociation constants, $K_d$'s, determined in the presence of 100 mM NaCl, 5 mM KCl, and 20 mM Tris-HCl, pH 7.4, are 0.10 ± 0.005, 0.046 ± 0.002, and 0.3 ± 0.02 pM for $K_v1.1$, $K_v1.2$, and $K_v1.3$, respectively. Under the same experimental conditions, ShK and ShK-Dap$^{22}$ cause concentration-dependent inhibition of $^{125}$I-HgTX$_1$A19Y/Y37F binding to each of these membrane preparations (Figure 4). In all cases, inhibition is monophasic, and Hill coefficients are close to 1. The calculated $K_i$ values for inhibition are presented in Table 1. ShK is a very potent inhibitor of $^{125}$I-HgTX$_1$A19Y/Y37F binding to both $K_v1.1$ and $K_v1.3$ mem-

Table 1[a]

| | $K_i$ (pM) | | |
|---|---|---|---|
| | $K_v$1.1 | $K_v$1.2 | $K_v$1.3 |
| ShK | 0.041 ± 0.001 | 5.03 ± 0.28 | 0.25 ± 0.005 |
| ShK-Dap$^{22}$ | 59 ± 2.5 | 20750 ± 1850 | 198 ± 5.5 |

[a] $^{125}$I-HgTX$_1$A19Y/Y37F binding to $K_v$1.1, $K_v$1.2, or $K_v$1.3 channels, in the absence or presence of either ShK or ShK-Dap$^{22}$, was determined as described in the text. $K_i$ values for inhibition were calculated as described under Experimental Procedures. Values represent the average ± SEM of three independent determinations, each one carried out in triplicate.

branes, with $K_i$'s of 0.041 and 0.25 pM, respectively, whereas it displays lower affinity, 5 pM, for $K_v$1.2. Substitution of diaminopropionic acid at Lys$^{22}$, ShK-Dap$^{22}$, decreases the potency of the peptide as an inhibitor of $^{125}$I-HgTX$_1$A19Y/Y37F binding to all three channels. The shift in affinity caused by this substitution is 1438-, 4122-, and 792-fold for $K_v$1.1, $K_v$1.2, and $K_v$1.3, respectively. Thus, it appears that $K_v$1.3 is the least affected by mutating Lys$^{22}$ in ShK, whereas the largest effects are observed with $K_v$1.2 channels.

Although electrophysiological experiments indicate that ShK-Dap$^{22}$ is ca. 20-fold more potent as an inhibitor of $K_v$1.3 than $K_v$1.1 channels (Figure 2), these differences are not observed in $^{125}$I-HgTX$_1$A19Y/Y37F equilibrium binding studies (Table 1). Although the ionic strength conditions of the binding assay, 100 mM NaCl and 5 mM KCl, can be considered similar to those of electrophysiological recordings, there are other differences between these assays that could contribute to the above results. For example, the occupancy by potassium of a binding site in the selectivity filter has been shown to cause destabilization of bound peptide in the outer vestibule (*28*, *31*). Because of the low potassium concentration, 5 mM, used in the above binding studies, $^{125}$I-HgTX$_1$A19Y/Y37F binding was carried out in the presence of 100 mM KCl, a condition that would be expected to lead to higher occupancy of ion binding sites in the selectivity filter. However, no difference in ShK-Dap$^{22}$ potency was found for either $K_v$1.1 or $K_v$1.3 under these conditions (data not shown). In addition, $K_v$1.1 was transiently expressed in TsA-201 cells with the same DNA construct used to transcribe mRNA for oocyte expression. Again, the potency of ShK-Dap$^{22}$ as an inhibitor of $^{125}$I-HgTX$_1$A19Y/Y37F binding was identical to that determined from stably transfected HEK cells (data not shown and Figure 4). Thus, in equilibrium binding studies with $^{125}$I-HgTX$_1$A19Y/Y37F, ShK-Dap$^{22}$ does not display specificity between $K_v$1.1 and $K_v$1.3 channels, and its affinity for $K_v$1.1 is higher than that determined in electrophysiological measurements.

*Binding of $^{125}$I-HgTX$_1$A19Y/Y37F to Heteromultimeric Channels: Effect of ShK and ShK-Dap$^{22}$.* Native brain $K_v$1 channels are mostly formed as heteromultimers. These channels contain mainly $K_v$1.2 subunit(s), with $K_v$1.1 coassociated in about 75% of the complexes (*3*, *16*, *18*, *32*, *33*). The stoichiometry and relative orientation of the $K_v$1.*x* subunits in the tetramers are not known. $^{125}$I-HgTX$_1$A19Y/Y37F binds to human brain membranes with high affinity and with a Hill coefficient of 1 (*18*). When binding of $^{125}$I-HgTX$_1$A19Y/Y37F is monitored in the presence of increasing concentrations of either ShK or ShK-Dap$^{22}$, a complex pattern of inhibition is observed (Figure 5A). Inhibition curves display Hill coefficients $\ll 1$ and most likely reflect the presence of subtypes of $^{125}$I-HgTX$_1$A19Y/Y37F receptors with different sensitivities to the peptides. The actual composition of the brain tetramers (i.e., the relative amounts of $K_v$1.1-sensitive to other insensitive subunits), and the spatial organization of the subunits (i.e., adjacent versus diagonal orientations), could be responsible for the observed complex inhibition patterns.

To study this in further detail, a $K_v$1.1-$K_v$1.2 dimer and a tetramer with all four subunits aligned in a single polypeptide, $K_v$1.1-$K_v$1.2-$K_v$1.1-$K_v$1.2, were transiently expressed in TsA-201 cells. $^{125}$I-HgTX$_1$A19Y/Y37F binds with high affinity to membranes derived from these cells with $K_d$'s of 0.10 ± 0.0046 and 0.039 ± 0.0012 pM for the $K_v$1.1-$K_v$1.2 dimer and the $K_v$1.1-$K_v$1.2-$K_v$1.1-$K_v$1.2 construct, respectively (data not shown). ShK and ShK-Dap$^{22}$ inhibit $^{125}$I-HgTX$_1$A19Y/Y37F binding to the $K_v$1.1-$K_v$1.2 dimer (Figure 5B) and to the $K_v$1.1-$K_v$1.2-$K_v$1.1-$K_v$1.2 tetrameric channel (Figure 5C), but the inhibition patterns are markedly different. For both types of heteromultimers, ShK displaces $^{125}$I-HgTX$_1$A19Y/Y37F binding with high potency, $K_i$'s of 0.081 ± 0.0037 (Figure 5B) and 0.028 ± 0.0003 pM (Figure 5C), respectively, and with Hill coefficients close to 1. In contrast, inhibition curves in the presence of ShK-Dap$^{22}$ are not monophasic and can be better fit by two binding components (Table 2). In the case of channels resulting from $K_v$1.1-$K_v$1.2 dimers, the high-affinity component of ShK-Dap$^{22}$ inhibition corresponds to ~29% of $^{125}$I-HgTX$_1$A19Y/Y37F binding sites, whereas for the $K_v$1.1-$K_v$1.2-$K_v$1.1-$K_v$1.2 channel, this component is close to 50% of the $^{125}$I-HgTX$_1$A19Y/Y37F receptors. It is interesting to note that the high-affinity site, $K_i$ of 0.35 pM (Table 2), corresponds to a receptor with >100-fold higher affinity for ShK-Dap$^{22}$ than the homomeric $K_v$1.1 channel, the more sensitive subunit of the $K_v$1.1-$K_v$1.2 complex. Thus, assembly of two $K_v$1 subunits with a 350-fold difference in ShK-Dap$^{22}$ sensitivity creates a new receptor site with much higher sensitivity than either channel alone. Under our experimental conditions, this effect can be observed with ShK-Dap$^{22}$ but not with ShK.

*Functional Consequences of Blocking $K_v$1.3 Channels: Membrane Potential Measurements.* An alternative functional assay for $K_v$1.3 channel activity is to measure changes in membrane potential with voltage-sensitive dyes (*34*, *35*). This voltage-sensitive dye system measures the change in fluorescence energy transfer between a coumarin dye anchored to the outside of the cell and a charged dye that is mobile within the membrane phase. Fluorescence emission from both dyes is measured, and a subsequent change in this ratio is proportional to the change that occurs in the membrane potential of the cells. A CHO cell line stably expressing the human $K_v$1.3 channel (ca. $10^5$ channels/cell) was used for the membrane potential assay. In this cell line, $K_v$1.3 sets the membrane potential, and block of this channel causes membrane depolarization (*36*). After addition of a $K_v$1.3 channel inhibitor to these cells, the membrane slowly depolarizes as monitored with the voltage-sensitive dye pair (data not shown). Activity of $K_v$1.3 can also be assayed after preincubation with an inhibitor by measuring the depolarization caused by addition of a high potassium solution (Figure 6). The decrease in potassium-induced depolarization reflects the degree to which the membrane had been previously depolarized by the $K_v$1.3 inhibitor. Preincubation for 1 h with increasing concentrations of MgTX causes a

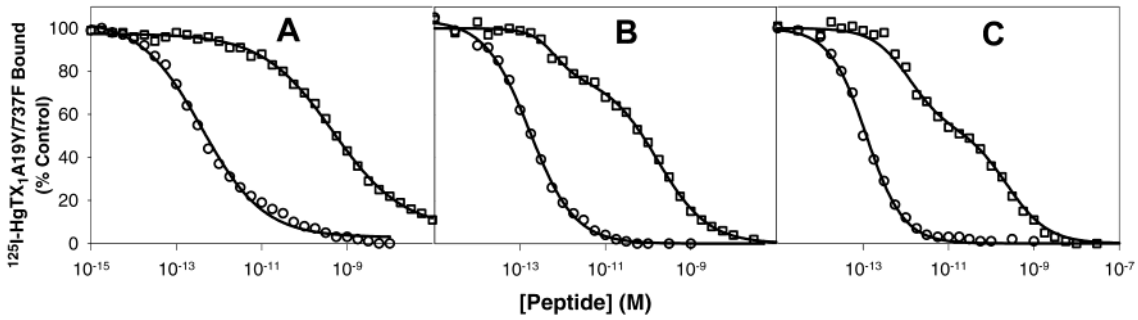


FIGURE 5: Binding of $^{125}$I-HgTX$_1$A19Y/Y37F to heteromultimeric $K_v1.x$ channels: effect of ShK and ShK-Dap$^{22}$. Membranes derived from human brain tissue (A) or TsA-201 cells transiently transfected with a $K_v1.1$-$K_v1.2$ dimer (B) or with a $K_v1.1$-$K_v1.2$-$K_v1.1$-$K_v1.2$ construct (C) were incubated with ~0.1 pM $^{125}$I-HgTX$_1$A19Y/Y37F, in the absence or presence of increasing concentrations of either ShK (○) or ShK-Dap$^{22}$ (□), for 20 h at room temperature. Specific binding data are presented relative to an untreated control. Data for ShK-Dap$^{22}$ in (B) and (C) were analyzed using a two binding site model as described under Experimental Procedures. Parameters derived from the curve fit are presented in Table 2.

Table 2 [a]

| | | ShK-Dap$^{22}$ | | |
|---|---|---|---|---|
| | ShK $K_i$ (pM) | $K_i$ (1) (pM) | no. of sites (1) (%) | $K_i$ (2) (pM) |
| $K_v1.1$-$K_v1.2$ dimer | 0.081 ± 0.003 | 0.35 ± 0.06 | 29 ± 1 | 85 ± 11.7 |
| $K_v1.1$-$K_v1.2$-$K_v1.1$-$K_v1.2$ | 0.029 ± 0.0003 | 0.35 ± 0.06 | 48 ± 0.8 | 54 ± 5.7 |

[a] $^{125}$I-HgTX$_1$A19Y/Y37F binding to $K_v1.1$-$K_v1.2$ dimer or $K_v1.1$-$K_v1.2$-$K_v1.1$-$K_v1.2$ channels, in the absence or presence of either ShK or ShK-Dap$^{22}$, was determined as described in the text. $K_i$ values for inhibition by ShK were calculated from the fit of the data to a one-site model. Binding parameters for inhibition by ShK-Dap$^{22}$ were calculated from the fit of the data to a two-site model as described under Experimental Procedures. Values represent the average ± SEM of three independent determinations, each one carried out in triplicate.

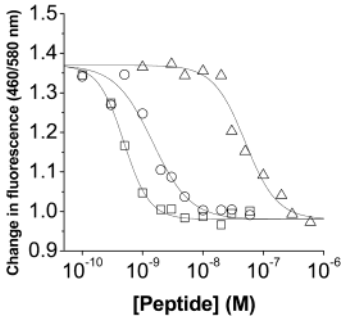


FIGURE 6: Membrane potential measurements in CHO cells stably transfected with $K_v1.3$. CHO cells stably expressing $K_v1.3$ were grown overnight in 96-well plates until confluent. The cells were stained with the CC2-DMPE dye for 30 min, washed, and incubated for 1 h with DiSBAC$_2$(3) dye, in the absence or presence of the indicated concentrations of peptide. The amount of depolarization caused by inhibition of $K_v1.3$ was assessed by measuring the membrane potential change after addition of 90 mM KCl. The data were fit to $IC_{50}$ values of 1.5, 0.51, and 50.4 nM for MgTX (○), ShK (□), and ShK-Dap$^{22}$ (△), respectively.

decrease in the potassium-induced depolarization with an $IC_{50}$ of 3.8 ± 3.1 nM ($n$ = 2). A similar potency, 0.56 ± 0.06 nM ($n$ = 2), was determined for ShK (Figure 6). Under identical conditions, ShK-Dap$^{22}$ is 100-fold weaker as a channel inhibitor, with an $IC_{50}$ of 71 ± 33 nM ($n$ = 2). The apparent potency of all three peptides is ca. 1000-fold lower than that observed in equilibrium binding experiments (Table 1 and data not shown). One possible explanation is that

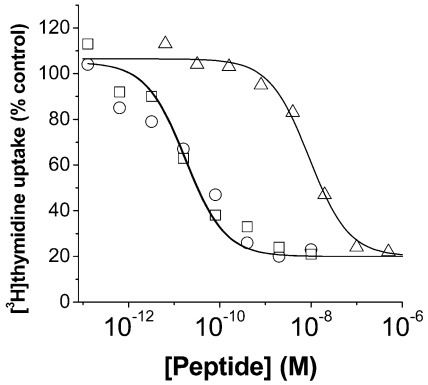


FIGURE 7: Inhibition of human T cell proliferation by ShK and ShK-Dap$^{22}$. Purified human T cells were stimulated with anti-CD3 and mononuclear blood cells in the absence or presence of increasing concentrations of either MgTX (○), ShK (□), or ShK-Dap$^{22}$ (△). Inhibition of [$^3$H]thymidine uptake was assessed relative to an untreated control. (○) $IC_{50}$ = 0.018 nM; (□) $IC_{50}$ = 0.017 nM; (△) $IC_{50}$ = 9 nM.

99.9% of the $K_v1.3$ channels need to be blocked before the cells depolarize, a consequence of the high channel density in this cell line. Since the mechanism for suppression of T-cell activation is presumably membrane depolarization due to $K_v1.3$ channel block, this assay indicates that ShK-Dap$^{22}$ is 100-fold less potent at depolarizing cells compared to ShK.

*Inhibition of Human T Cell Proliferation in Vitro by ShK and ShK-Dap$^{22}$.* In human T cells, blockade of the $K_v1.3$ channel suppresses T cell activation. It is believed that $K_v1.3$ sets the resting potential of human T cells and that channel inhibition causes cell depolarization, leading to attenuation in the T cell receptor mediated elevation of intracellular calcium that is necessary for T cell proliferation (*8*, *13*). When human T cells are stimulated with anti-CD3 and irradiated PBMC, there is a concentration-dependent inhibition of [$^3$H]thymidine uptake into human T cells by MgTX, ShK, and ShK-Dap$^{22}$ (Figure 7). Inhibition by all three peptides can be reversed by addition of conditioned medium from PHA-activated T cells, which contains a variety of cytokines. $IC_{50}$ values for inhibition by MgTX, ShK, and ShK-Dap$^{22}$ are 0.018, 0.017, and 9 nM, respectively. Thus, under our experimental conditions, ShK-Dap$^{22}$ is about 500-fold weaker than ShK in inhibiting human T cell proliferation, a process that depends on the activity of the $K_v1.3$ channel.

## DISCUSSION

The role that $K_v1.3$ channels play in the immune system has been the topic of many studies that have been prompted by the observation that $K_v1.3$ inhibitors attenuate the process of human T cell activation. On the basis of results from both in vitro and in vivo assays, $K_v1.3$ has been proposed to represent a therapeutic target for the prevention of graft rejection (*13*, *14*). More recently, $K_v1.3$ channels have also been proposed to play a critical role in autoimmune diseases. Thus, activated, myelin-reactive T ($T_{EM}$) cells from patients with multiple sclerosis express significantly higher levels of $K_v1.3$ channels than naive or central memory T cells, and $K_v1.3$ inhibitors suppress proliferation of $T_{EM}$ cells (*10*). To assess the therapeutic utility of modulating $K_v1.3$ channels in treatment of immune diseases, inhibitors with appropriate characteristics must be developed. In this context, ShK-Dap$^{22}$ was characterized as a potent and selective $K_v1.3$ inhibitor. Although ShK blocks $K_v1.1$ and $K_v1.3$ channels with similar high affinity, substitution of diaminopropionic acid at the critical Lys$^{22}$ residue was shown to have no effect on $K_v1.3$ inhibition but to significantly affect the peptide's potency on $K_v1.1$ channels (*6*). Thus, ShK-Dap$^{22}$ might have potential for being developed as a therapeutic agent. However, the results of the present study reveal a different profile for ShK-Dap$^{22}$ that suggests that its therapeutic utility may be compromised in vivo by the unexpected pharmacological properties of the peptide. In addition, a large body of evidence indicates that the potency of ShK-Dap$^{22}$ is significantly reduced when compared to ShK.

Initially both ShK and ShK-Dap$^{22}$ peptides were extensively characterized by analytical techniques, and the peptide content of the solutions was normalized by a number of techniques including amino acid sequencing, amino acid hydrolysis, and UV absorption. There are clear differences in the potency of these peptides against $K_v1.1$ and $K_v1.3$ channels, with ShK-Dap$^{22}$ displaying significantly lower affinity under all experimental conditions. In electrophysiological recordings of either human T cells or oocytes injected with human $K_v1.3$ mRNA, ShK-Dap$^{22}$ inhibits the $K_v1.3$ channel with a $K_i$ value of ~100 pM (Figures 1 and 2). Previously published values for inhibition of mouse or human $K_v1.3$ by ShK-Dap$^{22}$ range between 3.3 and 52 pM, with most values centered about 40 pM (*6*, *11*, *37*−*40*). Thus, the differences between our values and those of others could easily represent differences in the quantification of the mass of the peptides. It is also important to note that the $K_i$ values of ShK-Dap$^{22}$ for inhibition of $K_v1.1$ channels are not different between this (human) and previous (mouse) studies. The major discrepancy concerns the potency of the parent ShK peptide. In this study, we illustrate that ShK is a very potent, subpicomolar inhibitor of both $K_v1.1$ and $K_v1.3$ channels. Since development of steady-state block at low ShK concentrations requires incubation for long periods of time, we cannot exclude that the actual potency of ShK for these channels is even higher than reported in this study. We do not know for certain why the values in this study are different than those previously published (*6*, *11*, *37*, *38*, *40*, *41*), but we suspect these differences could be related to the time allowed for ShK to reach maximal block. Thus, the features of ShK and ShK-Dap$^{22}$ characterized in the present study are significantly different from those previously reported and strongly indicate that the potency of ShK is significantly altered after substituting diaminopropionic acid at Lys$^{22}$. It is interesting to note that the equivalent substitution in a related peptide, BgK, also leads to a marked loss in its potency against $K_v1.1$, $K_v1.2$, and $K_v1.3$ channels (*7*). There is, however, agreement in that ShK-Dap$^{22}$ displays selectivity between human $K_v1.1$ and $K_v1.3$ channels in electrophysiological recordings, although the difference is only ~20-fold. In other assays (see below), the peptide does not appear to preferentially interact with human $K_v1.1$ or $K_v1.3$ channels.

Differences between ShK and ShK-Dap$^{22}$ can also be observed in other types of assays that monitor the activity of $K_v1.3$ channels. $^{86}Rb^+$ flux assays monitoring $K_v1.3$ channels stably expressed in mammalian cells have been established and used to identify small molecule inhibitors of the channel (*16*, *19*). In this assay, both ShK and ShK-Dap$^{22}$ also display significant differences in their inhibitory activity. It is worth mentioning that the potencies of ShK and MgTX are most likely underestimated and limited by the actual concentration of $K_v1.3$ channels in the assay. To minimize this problem, the $K_v1.3$ concentration was decreased to a minimum that was technically acceptable for making accurate determinations. Even under these conditions, the potencies of ShK and MgTX may still reflect the concentration of $K_v1.3$ channels, and the peptides could be intrinsically more potent than what the assay indicates.

Members of the $K_v1$ channel family, such as $K_v1.1$, $K_v1.2$, and $K_v1.3$, are blocked by $HgTX_1$, and $^{125}$I-$HgTX_1$A19Y/Y37F binds with very high affinity (i.e., $K_i$'s <1 pM) to these channels (*18*). In $^{125}$I-$HgTX_1$A19Y/Y37F binding assays, ShK and ShK-Dap$^{22}$ also display very large differences of ca. 1000-fold in potency as inhibitors of peptide binding. The potency of ShK for both $K_v1.1$ and $K_v1.3$ is ≪1 pM, and in agreement with previous observations (*6*), the peptide is a weaker inhibitor of $K_v1.2$ channels. The present binding results do not agree with previously published data in which the potencies of ShK and ShK-Dap$^{22}$ as inhibitors of $^{125}$I-ChTX binding to $K_v1.3$ channels were evaluated and reported to be similar. It is most likely that the potency of ShK was underestimated in those studies because the receptor concentration that the authors used in the binding assay, 45 pM, is limiting (*6*). In the present binding assays, in which the incubation volume is 12 mL, the channel concentration is about 50 fM. This channel concentration could still limit the apparent observed potency, and ShK could have a higher intrinsic affinity for the $K_v1.1$ channel than that reported in this study. However, the data strongly indicate that the potency of ShK-Dap$^{22}$ is much lower than that of the parent peptide in these experimental protocols. There are some differences in the specificity of ShK-Dap$^{22}$ between electrophysiological and equilibrium binding experiments. In electrophysiology, the peptide is ~20-fold more potent in blocking $K_v1.3$ channels whereas such differences are not seen in the binding assays. These data suggest that the intrinsic affinity of ShK-Dap$^{22}$ for both channels is indeed the same but that, during ion conduction, either voltage-dependent conformational changes or differences in ion occupancy in the channel (*42*, *43*) affect the interaction of the peptide in the channel's outer vestibule.

The ability of $K_v1.3$ blockers to attenuate the $Ca^{2+}$-dependent process of human T cell activation in in vitro

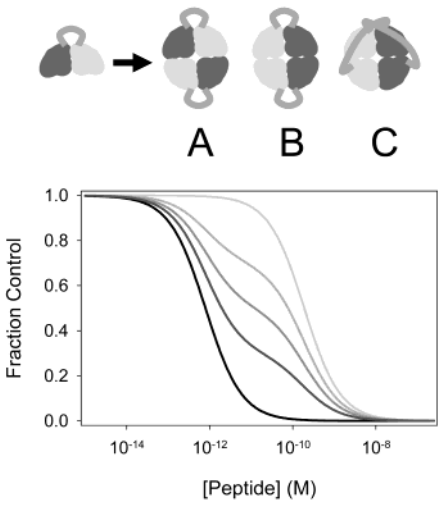


FIGURE 8: Heteromultimeric channels resulting from expression of a $K_v1.1$-$K_v1.2$ dimer. The predicted tetrameric subunit orientations A, B, and C after expression of a $K_v1.1$-$K_v1.2$ dimer construct are illustrated. The theoretical binding inhibition curves for a ligand that displays the same fold difference in affinity as ShK-Dap$^{22}$ for a $K_v1.1$-$K_v1.2$ dimer (Table 2) are illustrated. From left to right: (1) high-affinity configuration; (2−4) increasing fraction (0.3, 0.5, and 0.7) of low-affinity configuration; (5) low-affinity configuration. Experimental data from Figure 5B approximate the inhibition curve with a 0.7 ratio of low-affinity configuration.

assays has been used as an indication of the therapeutic utility of these agents. In these assays, ShK and ShK-Dap$^{22}$ also display markedly different potencies, although the concentrations that are needed to inhibit this process are higher than those predicted from electrophysiological experiments. The data are, however, consistent with the idea that a majority of channels must be blocked for cell depolarization to occur, which is necessary to prevent the rise in intracellular calcium that drives T cell activation (*8*, *13*). The membrane potential measurement assays, which use cells with a much larger density of $K_v1.3$ channels than present in T cells, confirm this idea and provide further evidence for the difference in potencies between the two ShK peptides.

The therapeutic window of any drug candidate is determined by the separation between its efficacy and adverse side effects. The concentrations of ShK-Dap$^{22}$ that are needed to prevent T cell activation also appear to affect other targets that would compromise the efficacy of the peptide as an immunosuppressant. For instance, the peptide displays an unexpected high affinity for some $K_v1.1$/$K_v1.2$ channel combinations that could be present in brain and peripheral tissues (*3*, *16*, *18*, *32*, *33*, *44*), and preliminary data indicate that the neurotoxicity of ShK-Dap$^{22}$ after ic injection in rats is only 2−3-fold lower than that of ShK (data not shown). This unexpected pharmacological behavior of ShK-Dap$^{22}$ has been observed in channels formed after expression of either a $K_v1.1$-$K_v1.2$ dimer or a $K_v1.1$-$K_v1.2$-$K_v1.1$-$K_v1.2$ tetrameric construct. It is intriguing that the combination of $K_v1.1$-sensitive and $K_v1.2$-insensitive channels leads to channels that are more sensitive (∼200-fold) to ShK-Dap$^{22}$ than either $K_v1.1$ or $K_v1.2$. As previously observed for expression of cyclic nucleotide-gated dimer channel constructs (*45*), three possible dimer−dimer configurations can lead to the formation of tetrameric channels (Figure 8). First, dimers can associate with the $K_v1.1$ subunit of one dimer contacting the $K_v1.2$ subunit of the other (tetramer A). Second, $K_v1.1$ and $K_v1.2$ subunits of each dimer can contact each other (tetramer B). Finally, the dimers could interlock to form channels, and the $K_v1.1$ and $K_v1.2$ subunits of each dimer, therefore, sit at opposite corners of the channel (tetramer C). The spatial orientation of the subunits in tetramers B and C is similar, and therefore two-thirds of the channels could have an identical pharmacological behavior. The present experimental data are consistent with the presence of one-third of high-affinity ShK-Dap$^{22}$ receptors and two-thirds of receptors that display identical affinity to $K_v1.1$ channels. Thus, the structural arrangement of the $K_v1.1$ with the insensitive $K_v1.2$ subunit in tetramer A provides additional binding energy for the peptide and reveals an unexpected pharmacological profile. Preferential interaction of ShK-Dap$^{22}$ with two adjacent subunits in $K_v1.3$ has been proposed from double-cycle mutant studies (*37*). However, our data appear to be more consistent with the peptide interacting with, at least, three of the channel subunits. Under the equilibrium binding conditions of our experiments, the two different ShK-Dap$^{22}$ binding affinities could not be due to two different orientations of the peptide in a homogeneous population of receptors because the high-affinity site will always prevail. Lower affinity orientations similar to those of homomultimeric $K_v1.2$ channels may exist but would not be revealed in these experiments. The results with the tetrameric construct are consistent with the idea that, in ∼50% of the channels, identical subunits are in a diagonally opposed orientation but they are adjacent to each other in the remaining 50% of the tetramers. It is interesting to note that ShK does not distinguish between the different $K_v1.1$-$K_v1.2$ channel combinations, as suggested by the monophasic inhibition curves that are observed with this peptide. However, we must emphasize that the experimental binding conditions do not allow the identification of inhibitors with $K_i$ values $\ll$0.04 pM and that it is technically impossible to make those determinations with the experimental tools that are currently available.

Human brain membranes represent a system where heteromultimeric channels of many different compositions exist (*16*). As suggested by the inhibition patterns of $^{125}$I-HgTX$_1$-A19Y/Y37F with ShK and ShK-Dap$^{22}$, the complexity of these tetramers is large. However, the data also illustrate two additional features. One is the difference in potencies between ShK and ShK-Dap$^{22}$ that has been observed consistently throughout this study. The other is that both peptides will be affecting native channels at much lower concentrations than those needed to inhibit T cell activation. Thus, these peptides do not appear to have the properties needed for therapeutic development. The search for $K_v1.3$ inhibitors with a good therapeutic window will be critical for their consideration as drug development candidates. Although some progress has been achieved in this area (*16*, *19*), more work is needed to optimize these molecules in order to achieve that goal.

## REFERENCES

1. Kaczorowski, G. J., and Garcia, M. L. (1999) *Curr. Opin. Chem. Biol. 3*, 448−458.
2. Beeton, C., Wulff, H., Singh, S., Botsko, S., Crossley, G., Gutman, G. A., Cahalan, M. D., Pennington, M., and Chandy, K. G. (2003) *J. Biol. Chem. 278*, 9928−9937.
3. Racape, J., Lecoq, A., Romi-Lebrun, R., Liu, J., Kohler, M., Garcia, M. L., Menez, A., and Gasparini, S. (2002) *J. Biol. Chem. 277*, 3886−3893.

4. Tudor, J. E., Pallaghy, P. K., Pennington, M. W., and Norton, R. S. (1996) *Nat. Struct. Biol. 3*, 317−320.
5. Dauplais, M., Lecoq, A., Song, J., Cotton, J., Jamin, N., Gilquin, B., Roumestand, C., Vita, C., Medeiros, C. L. C. d., Rowan, E. G., Harvery, A. L., and Menez, A. (1997) *J. Biol. Chem. 272*, 4302−4309.
6. Kalman, K., Pennington, M. W., Lanigan, M. D., Nguyen, A., Rauer, H., Mahnir, V., Paschetto, K., Kem, W. R., Grissmer, S., Gutman, G. A., Christian, E. P., Cahalan, M. D., Norton, R. S., and Chandy, K. G. (1998) *J. Biol. Chem. 273*, 32697−32707.
7. Alessandri-Harber, N., Lecoq, A., Gasparini, S., Grangier-Macmath, G., Jacquet, G., Harvey, A. L., Medeiros, C., Rowan, E. G., Gola, M., Menez, A., and Crest, M. (1999) *J. Biol. Chem. 274*, 35653−35661.
8. Leonard, R. J., Garcia, M. L., Slaughter, R. S., and Reuben, J. P. (1992) *Proc. Natl. Acad. Sci. U.S.A. 89*, 10094−10098.
9. Lin, C. S., Boltz, R. C., Blake, J. T., Nguyen, M., Talento, A., Fischer, P. A., Springer, M. S., Sigal, N. H., Slaughter, R. S., Garcia, M. L., Kaczorowski, G. J., and Koo, G. C. (1993) *J. Exp. Med. 177*, 637−645.
10. Wulff, H., Calabresi, P. A., Allie, R., Yun, S., Pennington, M., Beeton, C., and Chandy, K. G. (2003) *J. Clin. Invest. 111*, 1703−1713.
11. Beeton, C., Wulff, H., Barbaria, J., Clot-Faybesse, O., Pennington, M., Bernard, D., Cahalan, M. D., Chandy, K. G., and Beraud, E. (2001) *Proc. Natl. Acad. Sci. U.S.A. 98*, 13942−13947.
12. Beeton, C., Barbaria, J., Giraud, P., Devaux, J., Benoliel, A.-M., Gola, M., Sabatier, J. M., Bernard, D., Crest, M., and Beraud, E. (2001) *J. Immunol. 166*, 936−944.
13. Koo, G. C., Blake, J. T., Shah, K., Staruch, M. J., Dumont, F., Wunderler, D., Sanchez, M., McManus, O. B., Sirotina-Meisher, A., Fischer, P., Boltz, R. C., Goetz, M. A., Baker, R., Bao, J., Kayser, F., Rupprecht, K. M., Parsons, W. H., Tong, X.-C., Ita, I. E., Pivnichny, J., Vincent, S., Cunningham, P., Hora, D., Jr., Feeney, W., Kaczorowski, G., and Springer, M. S. (1999) *Cell. Immunol. 197*, 99−107.
14. Koo, G. C., Blake, J. T., Talento, A., Nguyen, M., Lin, S., Sirotina, A., Shah, K., Mulvany, K., Hora, D., Jr., Cunningham, P., Wunderler, D. L., McManus, O. B., Slaughter, R., Bugianesi, R., Felix, J., Garcia, M., Williamson, J., Kaczorowski, G., Sigal, N. H., Springer, M. S., and Feeney, W. (1997) *J. Immunol. 158*, 5120−5128.
15. Middleton, R. E., Bruguera, M., Bugianesi, R., Dai, G., Hwang, J., Jones, S., McManus, O., Sanchez, M., Slaughter, R., and Garcia, M. (2001) *Biophys. J. 80*, 438a.
16. Felix, J. P., Bugianesi, R. M., Schmalhofer, W. A., Borris, R., Goetz, M. A., Hensens, O. D., Bao, J.-M., Kayser, F., Parsons, W. H., Rupprecht, K., Garcia, M. L., Kaczorowski, G. J., and Slaughter, R. S. (1999) *Biochemistry 38*, 4922−4930.
17. Hanner, M., Schmalhofer, W. A., Green, B., Bordallo, C., Liu, J., Slaughter, R. S., Kaczorowski, G. J., and Garcia, M. L. (1999) *J. Biol. Chem. 274*, 25237−25244.
18. Koschak, A., Bugianesi, R. M., Mitterdorfer, J., Kaczorowski, G. J., Garcia, M. L., and Knaus, H.-G. (1998) *J. Biol. Chem. 273*, 2639−2644.
19. Schmalhofer, W. A., Bao, J., McManus, O. B., Green, B., Matyskiela, M., Wunderler, D., Bugianesi, R. M., Felix, J. P., Hanner, M., Linde-Arias, A.-R., Ponte, C. G., Velasco, L., Koo, G., Staruch, M. J., Miao, S., Parsons, W. H., Rupprecht, K., Slaughter, R. S., Kaczorowski, G. J., and Garcia, M. L. (2002) *Biochemistry 41*, 7781−7784.
20. Price, M., Lee, S. C., and Deutsch, C. (1989) *Proc. Natl. Acad. Sci. U.S.A. 86*, 10171−10175.
21. Hanson, D. C., Nguyen, A., Mather, R. J., Rauer, H., Koch, K., Burgess, L. E., Rizzi, J. P., Donovan, C. B., Bruns, M. J., Canniff, P. C., Cunningham, A. C., Verdries, K. A., Mena, E., Kath, J. C., Gutman, G. A., Cahalan, M. D., Grissmer, S., and Chandy, K. G. (1999) *Br. J. Pharmacol. 126*, 1707−1716.
22. Nguyen, A., Kath, J. C., Hanson, D. C., Biggers, M. S., Canniff, P. C., Donovan, C. B., Mather, R. J., Bruns, M. J., Rauer, H., Aiyar, J., Lepple-Wienhues, A., Gutman, G. A., Grissmer, S., Cahalan, M. D., and Chandy, K. G. (1996) *Mol. Pharmacol. 50*, 1672−1679.
23. Hill, R. J., Grant, A. M., Volberg, W., Rapp, L., Faltynek, C., Miller, D., Pagani, K., Baizman, E., Wang, S., Guiles, J. W., and Krafte, D. S. (1995) *Mol. Pharmacol. 48*, 98−104.
24. Mullmann, T. J., Munujos, P., Garcia, M. L., and Giangiacomo, K. M. (1999) *Biochemistry 38*, 2395−2402.
25. Giangiacomo, K. M., Sugg, E. E., Garcia-Calvo, M., Leonard, R. J., McManus, O. B., Kaczorowski, G. J., and Garcia, M. L. (1993) *Biochemistry 32*, 2363−2370.
26. Giangiacomo, K. M., Fremont, V., Mullmann, T. J., Hanner, M., Cox, R. H., and Garcia, M. L. (2000) *Biochemistry 39*, 6115−6122.
27. Giangiacomo, K. M., Garcia, M. L., and McManus, O. B. (1992) *Biochemistry 31*, 6719−6727.
28. Park, C.-S., and Miller, C. (1992) *Neuron 9*, 307−313.
29. Park, C.-S., and Miller, C. (1992) *Biochemistry 31*, 7749−7755.
30. Goldstein, S. A. N., and Miller, C. (1993) *Biophys. J. 65*, 1613−1619.
31. MacKinnon, R., and Miller, C. (1988) *J. Gen. Physiol. 91*, 335−349.
32. Scott, V. E. S., Muniz, Z. M., Sewing, S., Lichtinghagen, R., Parcej, D. N., Pongs, O., and Dolly, J. O. (1994) *Biochemistry 33*, 1617−1623.
33. Shamotienko, O. G., Parcej, D. N., and Dolly, J. O. (1997) *Biochemistry 36*, 8195−8201.
34. Gonzalez, J. E., and Tsien, R. Y. (1995) *Biophys. J. 69*, 1272−1280.
35. Gonzalez, J. E., and Tsien, R. Y. (1997) *Chem. Biol. 4*, 269−277.
36. DeFarias, F. P., Stevens, S. P., and Leonard, R. J. (1995) *Recept. Channels 3*, 273−281.
37. Lanigan, M. D., Kalman, K., Lefievre, Y., Pennington, M. W., Chandy, K. G., and Norton, R. S. (2002) *Biochemistry 41*, 11963−11971.
38. Rauer, H., Pennington, M., Cahalan, M., and Chandy, K. G. (1999) *J. Biol. Chem. 274*, 21885−21892.
39. Ghanshani, S., Wulff, H., Miller, M. J., Rohm, H., Neben, A., Gutman, G. A., Cahalan, M. D., and Chandy, K. G. (2000) *J. Biol. Chem. 275*, 37137−37149.
40. Chandy, K. G., Cahalan, M., Pennington, M., Norton, R. S., Wulff, H., and Gutman, G. A. (2001) *Toxicon 39*, 1269−1276.
41. Lanigan, M. D., Pennington, M. W., Lefievre, Y., Rauer, H., and Norton, R. S. (2001) *Biochemistry 40*, 15528−15537.
42. Zhou, Y., Morais-Cabral, J. H., Kaufman, A., and MacKinnon, R. (2001) *Nature 414*, 43−48.
43. Morais-Cabral, J. H., Zhou, Y., and MacKinnon, R. (2001) *Nature 414*, 37−42.
44. Suarez-Kurtz, G., Vianna-Jorge, R., Pereira, B. F., Garcia, M. L., and Kaczorowski, G. J. (1999) *J. Pharmacol. Exp. Ther. 289*, 1517−1522.
45. Morrill, J. A., and MacKinnon, R. (1999) *J. Gen. Physiol. 114*, 71−83.


BI035209E